

PERTURBATIONS OF THE LAMBDA-CDM MODEL IN A DYNAMICAL SYSTEMS PERSPECTIVE

ARTUR ALHO,^{1*} CLAES UGGLA,^{2†} AND JOHN WAINWRIGHT^{3‡}

¹*Center for Mathematical Analysis, Geometry and Dynamical Systems,*

Instituto Superior Técnico, Universidade de Lisboa,

Av. Rovisco Pais, 1049-001 Lisboa, Portugal.

²*Department of Physics, Karlstad University,*

S-65188 Karlstad, Sweden.

³*Department of Applied Mathematics, University of Waterloo,*

Waterloo, ON, N2L 3G1, Canada.

Abstract

The observational success and simplicity of the Λ CDM model, and the explicit analytic perturbations thereof, set the standard for any alternative cosmology. It therefore serves as a comparison ground and as a test case for methods which can be extended and applied to other cosmological models. In this paper we introduce dynamical systems and methods to describe linear scalar and tensor perturbations of the Λ CDM model, which serve as pedagogical examples that show the global illustrative powers of dynamical systems in the context of cosmological perturbations. This also allows us to compare perturbations with results in general relativity. Furthermore, we give a new approximation for the linear growth rate, $f(z) = \frac{d \ln \delta}{d \ln a} = \Omega_m^{\frac{6}{11}} - \frac{1}{70}(1 - \Omega_m)^{\frac{5}{2}}$, where z is the cosmological redshift, $\Omega_m = \Omega_m(z)$, while a is the background scale factor, and show that it is much more accurate than the previous ones in the literature.

1 Introduction

This paper is the first in a series of papers dealing with cosmological perturbations by means of dynamical systems formulations and methods. We will show how a wide variety of increasingly complex problems can be formulated as dynamical systems and how powerful dynamical systems methods can be applied to yield insights

*Electronic address: aalho@math.ist.utl.pt

†Electronic address: claes.uggla@kau.se

‡Electronic address: jwainwri@uwaterloo.ca

about cosmological perturbations. In particular, this will make it possible to apply approximation techniques from the theory of dynamical systems and to obtain illustrative pictures as well as mathematically rigorous results about the global structure of the various models solution spaces, thereby also providing a context for especially physically interesting solutions. Our aim is thus to provide a useful complement to traditional approaches to cosmological perturbations. Step by step we will introduce increasingly sophisticated models and methods. In this paper we focus on first order scalar and tensor perturbations of the spatially flat Λ CDM model with dust and a positive cosmological constant Λ . Since this model is mathematically simple and is compatible with a wide range of observations it is a natural choice as a first example to illustrate the most simple aspects of our dynamical systems approach to perturbative cosmology.

Dynamical systems have been used before to analyze cosmological linear scalar perturbations in general relativity (GR) with an open Robertson-Walker (RW) geometry as background, see [25] and references therein. These models turn out to be somewhat easier to handle than models with a spatially flat background,¹ which is what we will focus on. However, there has also been some previous work on dynamical systems in this area in GR, notably [4] which treated dust and radiation as a single fluid.

The main foundation for standard cosmology is the spatially flat RW geometry, characterized by a line element that can be written as

$$ds^2 = -dt^2 + a^2 \gamma_{ij} dx^i dx^j = a^2 (-d\eta^2 + \gamma_{ij} dx^i dx^j) = -H^{-2} dN^2 + a^2 \gamma_{ij} dx^i dx^j, \quad (1)$$

where $a(t)$ is the background scale factor, γ_{ij} is the flat spatial 3-metric, which in Cartesian coordinates is given by δ_{ij} , and $H = a^{-1} da/dt$ is the background Hubble variable. The different time coordinates above are the clock time t , the conformal time η , and the e -fold time

$$N = \ln x, \quad x = \frac{a}{a_0}, \quad (2)$$

where N describes the number of background e -foldings with respect to some reference epoch $a = a_0$ at which $x = 1$ (a negative N describes the number of e -folds before the reference time). If this reference epoch is the present time, then

$$x = \frac{1}{1+z}, \quad (3)$$

where z is the cosmological background redshift. Much of the work in cosmological perturbation theory uses the clock time t or the conformal time η , but we find it more convenient to use the e -fold time N as the starting point for our work.

The outline of the paper is as follows. In the next section we describe some aspects of the framework of our new dynamical systems approach to cosmological

¹In contrast to the spatially flat RW models, $\mathcal{H}^{-2} = (aH)^{-2}$, is always bounded for the spatially open models if the energy density is non-negative. This is due to how the spatial curvature term appears in the background Gauss constraint, which also can be used to solve for \mathcal{H}^{-2} . Since \mathcal{H}^{-2} appears in connection with the spatial derivatives of the perturbed equations, this significantly simplifies the analysis of the perturbed field equations in the open case.

perturbations. In Section 3 we consider linear scalar perturbations of the Λ CDM models from a dynamical systems perspective. We also present and discuss previously known analytic results in the present context. In addition we describe and discuss various asymptotic approximation methods and give a new more accurate approximation for the so-called linear growth rate. In Section 4 we consider the linear tensor perturbations from a dynamical systems perspective. In Section 5 we relate the present work to the full state space of GR. This is done by comparing asymptotic perturbative results with asymptotic results in GR for the Hubble-normalized comoving shear and Weyl tensor. The paper is concluded with some final remarks in Section 6.

2 Dynamical systems approach to cosmological perturbations

Our aim is to analyze cosmological perturbations by formulating the governing equations as *regular dynamical systems on compact state spaces*. In this paper we will consider first order scalar and tensor perturbations of the spatially flat Λ CDM models with dust and a positive cosmological constant Λ . However, since similar methods apply to models whose matter content consists of a perfect fluid with a barotropic equation of state and with or without a cosmological constant it is useful to point out some common features these models exhibit. The governing equation for scalar perturbations for this class of models can be a single second order partial differential equation (e.g. the Bardeen equation) or a system of two coupled first order partial differential equations (e.g. the Kodama-Sasaki equations), depending on the choice of gauge and the choice of variables, see e.g. [22]. For an arbitrary equation of state these governing equations will contain the spatial Laplacian \mathbf{D}^2 . This is also the case for the tensor perturbations which obey a linear second order differential master equation for a single variable.

In order to obtain ordinary differential equations (ODEs) we make a spatial Fourier decomposition of the perturbation variables, which involves replacing the perturbation variables by their Fourier coefficients and making the transition

$$\mathbf{D}^2 \rightarrow -k^2, \quad (4)$$

where k is the wave number. At this stage if we have a second order ODE as a governing equation we would replace it by a system of two coupled first order ODEs by using the first order time derivative as an independent variable. In this way the Einstein field equations for first order scalar and tensor perturbations of the models under consideration can be written as a system of linear ODEs of the form

$$u_1' = bu_1 + cu_2, \quad (5a)$$

$$u_2' = du_1 + eu_2, \quad (5b)$$

for two linear perturbation variables $u_1 = u_1(N, k^2)$ and $u_2 = u_2(N, k^2)$, where a $'$ denotes differentiation with respect to the e -fold time N . Due to the spatial Fourier decomposition one obtains complex variables, but thanks to that the differential equations are linear, real and complex parts satisfy the same equations, and

therefore we can without loss of generality consider u_1 and u_2 to be real, as are $b(N, k^2), c(N, k^2), d(N, k^2), e(N, k^2)$, whose specific form is determined by the background model. This is exemplified in detail in section 4 where tensor perturbations are treated.

The next step toward obtaining a regular dynamical system on a bounded state space is to introduce polar coordinates $u_1 = r \cos \theta, u_2 = r \sin \theta$, which thanks to the linearity of the equations lead to a decoupling of an equation for r and a reduction of the system of two linear ODEs (5) to one nonlinear ODE for $\theta(N, k^2)$:

$$\begin{aligned} \theta' &= d \cos^2 \theta + (e - b) \sin \theta \cos \theta - c \sin^2 \theta \\ &= \frac{1}{2}[(d - c) + (d + c) \cos 2\theta + (e - b) \sin 2\theta]. \end{aligned} \quad (6)$$

However, locally it is more convenient to replace θ with

$$y(N, k^2) = y := \tan \theta = u_2(N, k^2)/u_1(N, k^2), \quad (7)$$

which results in a Riccati ODE given by

$$y' = d + (e - b)y - cy^2, \quad (8)$$

which describes the essential “reduced” dynamics of the problem since, e.g., u_1 can be obtained as a quadrature from the decoupled equation $u_1' = u_1(b + cy)$ once the equation for y has been solved.

To obtain a dynamical system, i.e. a system of first order autonomous ODEs, that incorporates the dynamics described by the non-autonomous ODE (8) or (6), we introduce a new dependent variable $T = F(N)$, where F is a non-negative, bounded and increasing function. It follows that T satisfies an autonomous ODE of the form

$$T' = G(T), \quad \text{where} \quad G(T) = F'(F^{-1}(T)). \quad (9)$$

Note that $G(T)$ is obtained by differentiating $F(N)$ and then expressing N in terms T using the inverse function $N = F^{-1}(T)$. This equation is adjoined to (8) or (6), thereby yielding a 2-dimensional dynamical system for (y, T) or (θ, T) .

In practice, however, we have found it convenient to use the relation $N = \ln(x)$ to express $T = F(N)$ as a function of x rather than N . In particular we write T in terms of a subsidiary function $h(x)$ according to

$$T = \frac{h(x)}{1 + h(x)}, \quad (10)$$

where $h(x)$ is a non-negative, increasing, explicitly invertible, and suitably differentiable function which satisfies $h(0) = 0$ and $h(x) \rightarrow \infty$ when $x \rightarrow \infty$. This ensures that T is a non-negative, bounded and increasing function that satisfies $T(0) = 0$ and $\lim_{x \rightarrow \infty} T(x) = 1$. To find the function $G(T)$ in (9), differentiate (10) with respect to N using $dx/dN = x$ and then express x in terms of T using (10).

Augmenting the ODE (6) for θ with the ODE (9) for T yields the dynamical system

$$\theta' = d \cos^2 \theta + (e - b) \sin \theta \cos \theta - c \sin^2 \theta, \quad (11a)$$

$$T' = G(T), \quad (11b)$$

where the functions b, c, d, e are expressed as functions of T . The state space for this system is a finite cylinder in which all orbits (i.e., solution trajectories), begin at the boundary $T = 0$ and end at the boundary $T = 1$. We thus extend the state space to include these boundaries, which we refer to as the (extended) compactified *state space cylinder* $[0, 1] \times S^1$. Note that T can be regarded as a bounded time variable for which $T = 0$ and $T = 1$ correspond to $x = 0$ and $x \rightarrow \infty$, respectively.

As mentioned, for local analysis it is more convenient to use y instead of θ , which results in the system

$$y' = d + (e - b)y - cy^2, \quad (12a)$$

$$T' = G(T). \quad (12b)$$

In this representation traversing the infinite strip defined by $-\infty < y < \infty$ and $0 \leq T \leq 1$ twice corresponds to making one revolution on the state space cylinder $[0, 1] \times S^1$ with the global coordinates T and θ .²

The key to implementing the above procedure is to make an appropriate choice for the function $h(x)$ that determines the new dependent variable T through equation (10). In a particular application the choice is motivated by the form of the coefficient functions b, c, d, e in the initial system (5). We will use this procedure in the following sections to describe the scalar and tensor perturbations of the Λ CDM model.

3 Dynamical systems approach to scalar perturbations of Λ CDM

Linear scalar perturbations of a spatially flat RW background geometry can be described by

$$ds^2 = a^2 \left(-(1 + 2\phi)d\eta^2 + \mathbf{D}_i B d\eta dx^i + [(1 - 2\psi)\gamma_{ij} + 2\mathbf{D}_i \mathbf{D}_j C] dx^i dx^j \right), \quad (13)$$

where ϕ, B, ψ, C are the metric scalar perturbation variables (see e.g. Uggla and Wainwright (2018) [22].) The scalar matter perturbations for Λ CDM are given by the first order fractional matter density perturbation

$$\delta_m = \frac{{}^{(1)}\rho_m}{{}^{(0)}\rho_m}, \quad (14)$$

where the superscripts denote the order of the perturbation. The scalar velocity perturbation V is defined by the first order perturbation of the spatial *covariant* 4-velocity components according to the relation

$${}^{(1)}u_i = a\mathbf{D}_i V. \quad (15)$$

Setting $C = 0$ fixes the spatial gauge and covers most of the familiar gauges, although it excludes the synchronous gauge (for a recent work using the synchronous

²The reason for traversing the strip twice is that $y = u_2/u_1 = -u_2/(-u_1)$, i.e., the mapping is two-to-one, although note that the right hand side of (6) has a periodicity π .

gauge, see e.g. [8], and also [24] and [22] for further discussions and references). The temporal gauge can be fixed in a number of ways, e.g., by setting to zero one of the variables B , ψ , V , δ_m . We use the following terminology and subscripts to label the gauges:

- i) Poisson (Newtonian, longitudinal) gauge, subscript $_p$, defined by $B_p = 0$,
- ii) uniform curvature gauge, subscript $_c$, defined by $\psi_c = 0$,
- iii) total matter (comoving) gauge, subscript $_v$, defined by $V_v = 0$.

As shown in e.g. [22] each choice leads to a different system of governing equations. In particular, for linear perturbations the uniform (flat) curvature gauge leads to a simple system of two first order partial differential equations, which form a natural starting point for a dynamical systems analysis. We obtain this system of equations from [22], where it is given in the following form:³

$$(1 + q)\partial_N((1 + q)^{-1}\phi_c) = -c_s^2\mathcal{H}^{-2}\mathbf{D}^2(\mathcal{H}B_c), \quad (16a)$$

$$\partial_N(a^2 B_c) = -a^2\mathcal{H}^{-1}\phi_c, \quad (16b)$$

with

$$q' = -(1 + q)(1 + 3c_s^2 - 2q). \quad (17a)$$

Here q is the background deceleration parameter, defined by either of the following forms, $q = -\mathcal{H}'/\mathcal{H} = -(H'/H) - 1$. The background Einstein equations relate q to w according to ([22], equation (4)):

$$1 + q = \frac{3}{2}(1 + w). \quad (17b)$$

For the Λ CDM model we have⁴

$$c_s^2 = 0, \quad 1 + w = \Omega_m. \quad (18)$$

As basic perturbation variables for the Λ CDM model we choose $(u_1, u_2) = (\mathcal{H}B_c, -\phi_c)$, where we have scaled B_c with \mathcal{H} to obtain a dimensionless quantity, as discussed in [22] and [24]. We now specialize the governing equations (16) to the Λ CDM model, using equations (17) and (18). After expanding the ∂_N derivatives and replacing ∂_N by $'$ we obtain

$$\phi_c' = -3(1 - \Omega_m)\phi_c, \quad (19a)$$

$$(\mathcal{H}B_c)' = -\left(1 + \frac{3}{2}\Omega_m\right)(\mathcal{H}B_c) - \phi_c. \quad (19b)$$

Since the Laplacian \mathbf{D}^2 has dropped out, there is no need for a spatial Fourier decomposition. The system (19), which is of the form (5), constitutes the starting point for transforming the governing equations into a dynamical system.

³See equations (10), (54a) and (54b) in [22]. We have dropped superscripts ⁽¹⁾ on the perturbation variables, and have set $\Gamma = 0$ since we are considering a barotropic fluid.

⁴See, for example, [22], Appendix B.

We now digress to describe the background dynamics of the Λ CDM model in order to obtain the x -dependence of Ω_m . The density parameters are given by

$$\Omega_m = \Omega_{m0} x^{-1} \left(\frac{\mathcal{H}_0}{\mathcal{H}} \right)^2, \quad \Omega_\Lambda = \Omega_{\Lambda 0} x^2 \left(\frac{\mathcal{H}_0}{\mathcal{H}} \right)^2, \quad (20)$$

which implies that

$$\frac{\Omega_\Lambda}{\Omega_m} = \lambda_m x^3, \quad \text{where} \quad \lambda_m := \frac{\Omega_{\Lambda 0}}{\Omega_{m0}} = \frac{\Lambda}{\rho_{m0}}. \quad (21)$$

Since $\Omega_m + \Omega_\Lambda = 1$ it follows from (21) that

$$\Omega_m = \frac{1}{1 + \lambda_m x^3}. \quad (22)$$

3.1 Derivation of the dynamical systems

The metric perturbations in the uniform curvature gauge

We have shown that perturbations of the Λ CDM model are described by the system of ODEs (19) which we repeat here:

$$\phi_c' = -3(1 - \Omega_m)\phi_c, \quad (23a)$$

$$(\mathcal{H}B_c)' = -\left(1 + \frac{3}{2}\Omega_m\right)(\mathcal{H}B_c) - \phi_c, \quad (23b)$$

with variables $(u_1, u_2) = (\mathcal{H}B_c, -\phi_c)$. This problem is explicitly solvable, and we will later give the solution. Here, however, we will use it as a first illustration of our dynamical systems approach. We therefore introduce $y = u_2/u_1$, as in (7), but give y a subscript, y_c , as a reminder that we are using the uniform curvature gauge, thus

$$y_c = \frac{-\phi_c}{\mathcal{H}B_c}. \quad (24)$$

It follows from (23) that

$$y_c' = y_c \left(\frac{5}{2} - \frac{9}{2}(1 - \Omega_m) - y_c \right). \quad (25)$$

To complete the process of constructing a dynamical system we now have to make a choice for the additional independent variable T . It follows from equation (22) that

$$1 - \Omega_m = \frac{\lambda_m x^3}{1 + \lambda_m x^3} = \Omega_\Lambda, \quad (26)$$

which suggests that we choose⁵

$$T = \frac{\lambda_m x^3}{1 + \lambda_m x^3} = 1 - \frac{1}{1 + \lambda_m x^3} = \Omega_\Lambda. \quad (27)$$

⁵The second expression is useful for the calculation that follows.

In other words the function $h(x)$ in (10) is given by $h(x) = \lambda_m x^3$, which has the desired properties. Differentiating (27) with respect to N yields

$$T' = \frac{3\lambda_m x^3}{(1 + \lambda_m x^3)^2} = 3T(1 - T), \quad (28)$$

after expressing x in terms of T using (27) again. This is the desired autonomous ODE for T . Note that $0 \leq T \leq 1$ and that $T(x)$ is an increasing function, as required. We finally express the coefficient $1 - \Omega_m$ in equation (25) in terms of T . The resulting equation, with (28), comprises the desired (analytic) dynamical system as follows:

$$y_c' = y_c \left(\frac{5}{2} - \frac{9}{2}T - y_c \right), \quad (29a)$$

$$T' = 3T(1 - T). \quad (29b)$$

Since y_c is defined by the ratio of two metric coefficients, one orbit (i.e., solution trajectory) of the above system corresponds to a one-parameter family of solutions. Furthermore, the solutions for the dynamical system (29) correspond to solutions with all possible (non-zero) values of λ_m since λ_m is incorporated in the definition of T . In order to solve for $y_c(N, x^i)$ one has to impose an initial condition at $N = 0$, which corresponds to the initial epoch $a = a_0$, of the form $y_c(0, x^i) = f(x^i)$, where $f(x^i)$ is an arbitrary spatial function. Note that the initial value of $T(N)$, where $T(N)$ was chosen in order to arrive at a simple form for (29) and is given by (27), is $T(0) = 1 - \Omega_{m0}$ where Ω_{m0} is the initial value of $\Omega_m(N)$.

Finally we note that the full dynamical system in the uniform curvature consists of the state space vector $(\mathcal{H}B_c, \phi_c, T)$ governed by the equations (23) and (29b). This state space can then be covered by using polar coordinates $\mathcal{H}B_c = r_c \cos \theta_c$, $-\phi_c = r_c \sin \theta_c$, which leads to a decoupling of r_c from a dynamical system with a reduced state space vector (θ_c, T) . Locally it is, however, more convenient to use $y_c(N, x^i)$, and $\mathcal{H}B_c(N, x^i)$ as the decoupled variable, which obeys the equation

$$(\mathcal{H}B_c)' = \left(y_c - \frac{5}{2} + \frac{3}{2}T \right) (\mathcal{H}B_c), \quad (30)$$

which is easily solved as a quadrature once a solution $y_c(N, x^i), T(N)$ has been obtained, thereby also yielding the second constant of the motion which together with the constant of the motion for the reduced system for (y_c, T) characterizes the various scalar perturbations.

The fractional density perturbation in the total matter gauge

The density contrast δ is defined by

$$\delta = \frac{{}^{(1)}\rho_m}{{}^{(0)}\rho_m}, \quad (31)$$

where ${}^{(0)}\rho_m$ is the background matter density and ${}^{(1)}\rho_m$ is the linear density perturbation. The comoving density contrast δ_v , the gauge invariant that equals δ in the total matter/comoving gauge, plays a central role in observational cosmology.

Since δ_v satisfies a second order evolution equation we can apply our method to analyze its behaviour from a dynamical systems perspective. In the Λ CDM universe this evolution equation has the following form when using e -fold time N :⁶

$$\delta_v'' + \left(2 - \frac{3}{2}\Omega_m\right)\delta_v' - \frac{3}{2}\Omega_m\delta_v = 0. \quad (32)$$

In order to formulate this differential equation as a dynamical system we use $(u_1, u_2) = (\delta_v', \delta_v)$ as basic variables, and define

$$y_v = \frac{\delta_v'}{\delta_v}, \quad (33)$$

in accordance with equation (7).

We obtain the ODE for y_v by differentiating (33) using (32), and we make the same choice (27) of T as before. This results in the following dynamical system

$$y_v' = \frac{3}{2}(1 - T) - \frac{1}{2}(1 + 3T)y_v - y_v^2, \quad (34a)$$

$$T' = 3T(1 - T). \quad (34b)$$

This formulation of the evolution equations which is based on $y_v = \delta_v'/\delta_v$ differs from the system that is based on $y_c = -\phi_c/\mathcal{H}B_c$. However, y_c and y_v are closely related, as will be shown later.

3.2 Dynamical systems analysis

In this section we use dynamical systems methods to obtain qualitative information about the family of all solutions of the perturbed field equations, including asymptotic descriptions of the solutions at early and late times.

The uniform curvature gauge

When using the uniform curvature gauge the differential equations that define the reduced dynamical system are given by equations (29), which we here repeat for the reader's convenience:

$$y_c' = y_c \left(\frac{5}{2} - \frac{9}{2}T - y_c \right), \quad (35a)$$

$$T' = 3T(1 - T). \quad (35b)$$

The associated state space is the infinite strip:

$$-\infty < y_c < \infty, \quad 0 \leq T \leq 1, \quad (36)$$

⁶This evolution equation has been given in a general context in Uggla and Wainwright (2018) [22], equation (71a.b). When specialized to Λ CDM and to first order perturbations, equation (71a) reads $\mathcal{L}_D\delta_v = 0$, where the differential operator \mathcal{L}_D in (71b) reduces to $\mathcal{L}_D = \partial_N^2 + (1 - q)\partial_N - (1 + q)$. Since $1 + q = \frac{3}{2}(1 + w) = \frac{3}{2}\Omega_m$ we obtain our equation (31). To avoid confusion we note that the usual density contrast δ is defined by normalizing with $^{(0)}\rho_m$, while δ in [22] is defined by normalizing with $^{(0)}\rho + ^{(0)}p$. In the Λ CDM universe these two normalizations are the same (see [22], Appendix B).

with boundaries $T = 0$ and $T = 1$. Alternatively we can use the angular variable θ_c defined by $y_c = \tan \theta_c$, which yields the reduced regular global state space which is a finite section of a cylinder $[0, 1] \times S^1$, as discussed in section 2.

The analysis of this dynamical system is straightforward. Equation (35b) shows that all the fixed points of the system lie on the boundaries $T = 0$ and $T = 1$, and that each orbit is past asymptotic to a fixed point on $T = 0$ and future asymptotic to a fixed point on $T = 1$. The local stability of the fixed points can be determined in the usual way by linearizing the differential equations.

When specialized to the $T = 0$ and $T = 1$ boundaries the differential equation (35a) results in the following equations:

$$y'_c|_{T=0} = y_c \left(\frac{5}{2} - y_c \right), \quad (37a)$$

$$y'_c|_{T=1} = -y_c(2 + y_c). \quad (37b)$$

It follows that on the $T = 0$ boundary there are two fixed points (four in the case of θ_c , although they are connected by the discrete symmetry $\theta \rightarrow \theta + \pi$ and thereby given by the two fixed points for y_c):⁷

$$P_{0+}: \quad y_c = \frac{5}{2}; \quad \theta_c = \arctan \frac{5}{2} + n\pi, \quad (38a)$$

$$P_{0-}: \quad y_c = 0; \quad \theta_c = n\pi. \quad (38b)$$

Linearization shows that the fixed point P_{0+} is a hyperbolic saddle and that a single orbit originates from P_{0+} and is future asymptotic to the $T = 1$ boundary. To obtain an analytical approximation for this special orbit, we make a series expansion for y_c in powers of T and use the system (29) to solve for the coefficients,⁸ which leads to

$$\begin{aligned} y_c &= \frac{5}{2} - \frac{3^2 \cdot 5}{2 \cdot 11} T - \frac{2 \cdot 3^3 \cdot 5}{11^2 \cdot 17} T^2 + \dots \\ &= \frac{5}{2} - \frac{3^2 \cdot 5}{2 \cdot 11} \lambda_m x^3 + \frac{3^2 \cdot 5^3 \cdot 7}{2 \cdot 11^2 \cdot 17} (\lambda_m x^3)^2 + \dots, \end{aligned} \quad (39)$$

for T and x close to zero. Next, linearization shows that the fixed point P_{0-} is a hyperbolic source, and hence a one-parameter family of orbits originates from P_{0-} . A series expansion in T results in

$$\begin{aligned} y_c &= C_0 T^{\frac{5}{6}} \left(1 - \frac{2}{3} T \right) - \frac{2}{5} C_0^2 T^{\frac{5}{3}} + \dots \\ &= C_0 (\lambda_m x^3)^{\frac{5}{6}} \left(1 - \frac{3}{2} \lambda_m x^3 \right) - \frac{2}{5} C_0^2 (\lambda_m x^3)^{\frac{5}{3}} + \dots, \end{aligned} \quad (40)$$

where C_0 is a spatial function that parameterizes the orbits depending on the spatial position.

Inserting the series expansion (40) into equation (30) for $\mathcal{H}B_c$ shows that $\mathcal{H}B_c \rightarrow \infty$ toward the past for all orbits that originate from P_{0-} (to leading order it suffices to insert $y_c = 0$ into (30)). In contrast inserting (39) into (30) shows that $\mathcal{H}B_c$ is finite asymptotically for the orbit that originates from P_{0+} . Since $\mathcal{H}B_c = -\psi_p$ (see equation (61) below), it follows that the orbit that originates from P_{0+} is the only

⁷The first subscript on a fixed point P denotes the value of T while the + (-) denotes the larger (smaller) value of y_c .

⁸This can be mathematically justified by relating this series expansion to a so-called Picard expansion, see e.g. [18] and references therein.

orbit along which the perturbations remain finite into the past i.e. as $T \rightarrow 0$. Below we will identify this orbit with the so-called growing mode solution toward the future. Along all other orbits into the past, i.e., solutions that originate from P_{0-} , (some of) the perturbations increase without bound and hence will not asymptotically approximate solutions of the full Einstein equations. This is related to the fact that a general solution of the perturbed Einstein equations for scalar Λ CDM perturbations is a linear combination of a so-called *growing mode* and a *decaying mode*, where the latter has the property that it becomes unbounded into the past.

On the $T = 1$ boundary it follows from (37b) that the fixed points are given by

$$P_{1+}: \quad y_c = 0; \quad \theta_c = n\pi, \quad (41a)$$

$$P_{1-}: \quad y_c = -2; \quad \theta_c = n\pi - \arctan 2. \quad (41b)$$

Linearization shows that the fixed point P_{1-} is a hyperbolic saddle that attracts a single orbit that is past asymptotic to $T = 0$. A series expansion in $1 - T$ yields:

$$\begin{aligned} y_c &= -2 + \frac{3^2}{5}(1 - T) + \frac{3^3}{24 \cdot 5^2}(1 - T)^2 + \dots \\ &= -2 + \frac{3^2}{5}(\lambda_m x^3)^{-1} - \frac{3^2 \cdot 7 \cdot 11}{24 \cdot 5^2}(\lambda_m x^3)^{-2} + \dots \end{aligned} \quad (42)$$

Finally, linearization shows that the fixed point P_{1+} is a hyperbolic sink, which implies that a one-parameter family of orbits is asymptotic to P_{1+} . A series expansion in $1 - T$ results in

$$\begin{aligned} y_c &= C_1(1 - T)^{\frac{2}{3}}(1 - \frac{5}{6}(1 - T)) + \frac{1}{2}C_1^2(1 - T)^{\frac{4}{3}} + \dots \\ &= C_1(\lambda_m x^3)^{-\frac{2}{3}}(1 - \frac{3}{2}(\lambda_m x^3)^{-1}) + \frac{1}{2}C_1^2(\lambda_m x^3)^{-\frac{4}{3}} + \dots, \end{aligned} \quad (43)$$

where C_1 is a spatial function that parameterizes the orbits depending on the spatial position.

The preceding analysis of the stability of the fixed points enables one to predict the qualitative form of the state space (36) in figure 1 which shows the fixed points, the special heteroclinic orbits (i.e. solution trajectories that originate and end at two distinct fixed points), $P_{0-} \rightarrow P_{1-}$, $P_{0-} \rightarrow P_{1+}$ (note that equation (35a) shows that this orbit is the invariant set $y_c = 0$, which in turn corresponds to the invariant set $\phi_c = 0$ of equation (23a)), and $P_{0+} \rightarrow P_{1+}$, together with some typical orbits of the dynamical system. The most significant aspect of the state space in figure 1 is the heteroclinic orbit $P_{0+} \rightarrow P_{1+}$, the growing mode solution, which represents the most physically important solution of the perturbation equations (actually a one parameter family of solutions), and which thereby is the primary focus in cosmological perturbation theory.

As a final side remark we note the following about the heteroclinic growing mode orbit $P_{0+} \rightarrow P_{1+}$. Since P_{0+} is a saddle point *and* P_{1+} is a local sink, this orbit acts as an “attractor solution” toward the future of nearby orbits, reminiscent of “attractor solutions” in inflationary cosmology. The latter, however, are associated with a non-hyperbolic saddle point, whose unstable manifold is a center manifold, rather than a hyperbolic saddle point, which allows the inflationary regime to last longer than it would if the saddle was hyperbolic, see e.g. [2] for a discussion of attractor solutions in inflationary cosmology.

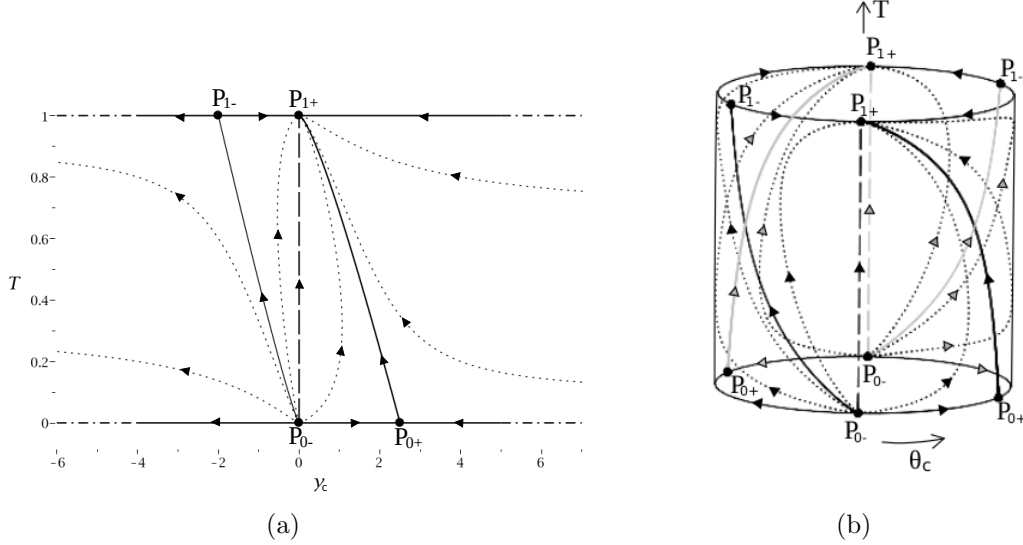


Figure 1: Solution structure for scalar perturbations of Λ CDM cosmology in the uniform (flat) curvature gauge, where $y_c = \tan \theta_c = -\phi_c/\mathcal{H}B_c$, and $T = 1 - \Omega_m = \Omega_\Lambda$. The $P_{0+} \rightarrow P_{1+}$ solution is the growing mode solution.

The comoving density perturbation

The dynamical system based on the comoving density contrast $y_v = \delta'_v/\delta_v$ is given by (34), which we repeat here:

$$y'_v = \frac{3}{2}(1-T) - \frac{1}{2}(1+3T)y_v - y_v^2, \quad (44a)$$

$$T' = 3T(1-T). \quad (44b)$$

The structure of the orbits of this system is very similar to that of the system (35), with the fixed points lying on the boundaries $T = 0$ and $T = 1$.

When specialized to these boundaries the differential equation (44a) results in the following equations:

$$y'_v|_{T=0} = \frac{1}{2}(1-y_v)(3+2y_v), \quad (45a)$$

$$y'_v|_{T=1} = -y_v(2+y_v). \quad (45b)$$

It follows that on the $T = 0$ ($x = 0$) boundary the fixed points are given by

$$P_{0+}: \quad y_v = 1; \quad \theta_v = \frac{\pi}{4} + n\pi, \quad (46a)$$

$$P_{0-}: \quad y_v = -\frac{3}{2}; \quad \theta_v = -\arctan \frac{3}{2} + n\pi. \quad (46b)$$

Linearization shows that the fixed point P_{0-} is a hyperbolic source, while the hyperbolic saddle P_{0+} has a single orbit originating from it into the interior, which, as we will see, describes the growing mode solution. A series expansion for this orbit yields

$$\begin{aligned} y_v &= 1 - \frac{2 \cdot 3}{11}T - \frac{2 \cdot 3^3 \cdot 5}{11^2 \cdot 17}T^2 + \dots \\ &= 1 - \frac{2 \cdot 3}{11}\lambda_m x^3 + \frac{2^2 \cdot 3 \cdot 71}{11^2 \cdot 17}(\lambda_m x^3)^2 + \dots \end{aligned} \quad (47)$$

On the $T = 1$ boundary the fixed points are given:

$$P_{1+}: \quad y_v = 0; \quad \theta_v = n\pi, \quad (48a)$$

$$P_{1-}: \quad y_v = -2; \quad \theta_v = -\arctan 2 + n\pi. \quad (48b)$$

The fixed point P_{1+} is a hyperbolic sink, while the fixed point P_{1-} is a hyperbolic saddle which attracts a single interior orbit.

There is a one-to-one correspondence as regards fixed points and stability properties between the dynamical system (44) and the dynamical system (35) for the state space (y_c, T) . This correspondence is reflected in the similarity between the form of the orbits in figure (1a) and figure (2a).⁹ In particular the heteroclinic orbit $P_{0+} \rightarrow P_{1+}$ again represents solutions that only contain the growing mode. Moreover, since y_v is positive on this orbit and $y_v = \delta'_v/\delta_v$ it follows that when $\delta_v > 0$ then δ_v is growing throughout its evolution (hence the name, growing mode), although δ_v approaches a constant value toward the future since $y_v = 0$ at P_{1+} .¹⁰ Finally, the comoving density contrast y_v for the growing mode solution is often referred to as the linear growth rate, which we will denote as $f(z)$ when expressed in terms of the redshift z .

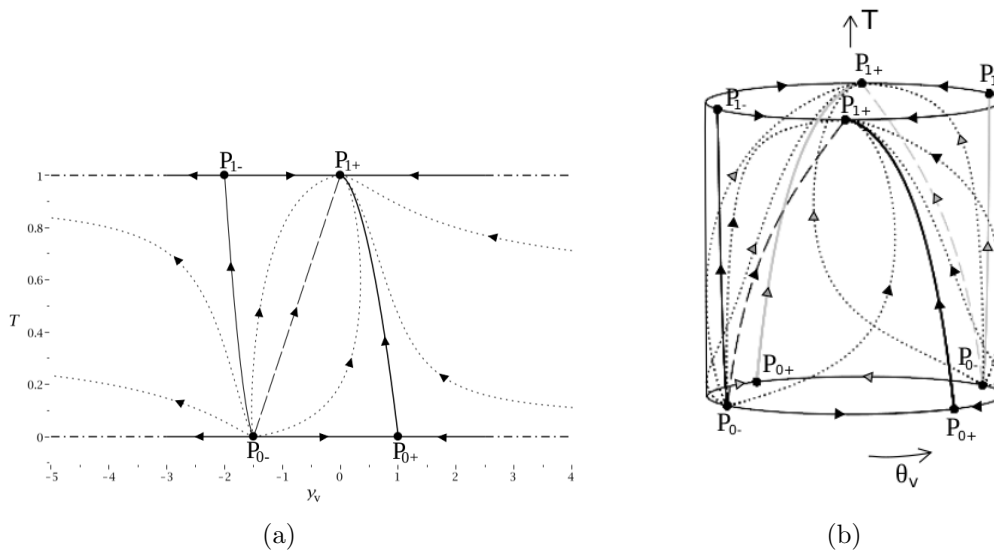


Figure 2: Global solution structure for $y_v = \delta'_v/\delta_v$ in Λ CDM cosmology, where $T = 1 - \Omega_m = \Omega_\Lambda$ is a monotonically increasing function in the background scale factor. The $P_{0+} \rightarrow P_{1+}$ orbit describes the growing mode solution.

In the above discussion of y_v we have refrained from giving details about asymptotics, except for the growing mode solution. The reason for this is that y_v and y_c can be related to each other, as shown in the next section about explicit solutions.

⁹Just before submitting the present paper, Basilakos *et al.* published a paper [3] on the archive with a diagram that corresponds to figure (2a), but with Ω_m instead of $T = 1 - \Omega_m$. They also gave the explicit solution (their equation (21)) for y_v , which in their notation was called U_m , but in a less transparent form than that given in the next section.

¹⁰An analogue of the orbit $y_c = 0$ in figure (1a) also occurs in figure (2a). It is the heteroclinic orbit $P_{0-} \rightarrow P_{1+}$ and it is given by $y_v = -(3/2)(1 - T)$.

This will also establish the identification of the growing mode orbits in the $y_c - T$ and $y_v - T$ state spaces.

3.3 Explicit solutions

In this section we derive and discuss the explicit solutions for y_c and y_v as functions of the time variable T . For the variable $y_c = -\phi_c/(\mathcal{H}B_c)$ we begin with the governing equations (16) in the uniform curvature gauge, which when applied to the Λ CDM universe simplify to

$$\partial_a((1+q)^{-1}\phi_c) = 0, \quad (49a)$$

$$\partial_a(a^2 B_c) = -a\mathcal{H}^{-1}\phi_c, \quad (49b)$$

where ∂_a refers to the partial derivative with respect to the background scale factor a . We can successively solve the equations to obtain

$$\phi_c = (1+q)C_+, \quad (50a)$$

$$\mathcal{H}B_c = -g(a)C_+ + \mathcal{H}a^{-2}C_-. \quad (50b)$$

where C_+ , C_- are arbitrary spatial functions and¹¹

$$g(a) := \frac{\mathcal{H}}{a^2} \int_0^a \frac{\bar{a}}{\mathcal{H}} (1+q) d\bar{a}. \quad (51)$$

In order to obtain y_c as a function of T we need to express ϕ_c and $\mathcal{H}B_c$ as functions of T , using equations (20)-(22), (27) and (29b). The results are as follows:¹²

$$\phi_c = -(1-T)C_+, \quad \mathcal{H}B_c = T^{-\frac{5}{6}}(1-T)^{\frac{1}{3}}(C_+I + C_-), \quad (52)$$

where¹³

$$I(T) = \frac{1}{3} \int_0^T \bar{T}^{-\frac{1}{6}} (1-\bar{T})^{-\frac{1}{3}} d\bar{T}. \quad (53)$$

It follows that the variable $y_c = -\phi_c/(\mathcal{H}B_c)$ is given by

$$y_c = \frac{C_+ T^{\frac{5}{6}} (1-T)^{\frac{2}{3}}}{C_+ I + C_-}. \quad (54)$$

The function $I(T)$ is well-defined at the end points,

$$I(0) = 0, \quad I(1) = I_1 = \frac{1}{3} \int_0^1 \bar{T}^{-\frac{1}{6}} (1-\bar{T})^{-\frac{1}{3}} d\bar{T}. \quad (55)$$

¹¹See section 7 in [23] for properties and a discussion about the perturbation evolution function $g(a)$.

¹²As intermediate steps we obtain $\mathcal{H}/a^2 = CT^{-5/6}(1-T)^{-1/3}$, $1+q = \frac{3}{2}(1-T)$, and $d\bar{a}/\bar{a} = dT/(3T(1-T))$. Here C is a constant that does not appear in the final result. The constants C_{\pm} in (50) have been redefined in obtaining (52).

¹³ $I(T)$ is related to g when expressed in terms of T according to $g(T) = \frac{3}{2}T^{-\frac{5}{6}}(1-T)^{\frac{1}{3}}I(T)$.

and the leading order behaviour of $I(T)$ is given by the following limits:

$$\lim_{T \rightarrow 0} \frac{I(T)}{T^{5/6}} = \frac{2}{5}, \quad \lim_{T \rightarrow 1} \frac{I(T) - I_1}{(1 - T)^{2/3}} = -\frac{1}{2}. \quad (56)$$

We can now relate the explicit solution (54) to the orbits of the dynamical system in figure 1. It follows from (54) that there are two special values of C_- , namely $C_- = 0$ and $C_- = -C_+I_1$ that affect the limit of y_c as $T \rightarrow 0, 1$, as follows:

$$\lim_{T \rightarrow 0} y_c = \frac{5}{2}, \quad \text{if } C_- = 0, \quad \lim_{T \rightarrow 0} y_c = 0, \quad \text{if } C_- \neq 0, \quad (57a)$$

$$\lim_{T \rightarrow 1} y_c = -2, \quad \text{if } C_- = -C_+I_1, \quad \lim_{T \rightarrow 1} y_c = 0, \quad \text{if } C_- \neq -C_+I_1. \quad (57b)$$

Referring to figure 1 we conclude that the orbit with $C_- = 0$ is the growing mode orbit, *i.e.* the orbit that is past asymptotic to the fixed point P_{0+} , while the orbits with $C_- \neq 0$ are those that are past asymptotic to the local source P_{0-} . Further, the orbit with $C_- = -C_+I_1$ is the special orbit that is future asymptotic to the fixed point P_{1-} , while the orbits with $C_- \neq -C_+I_1$ are those that are future asymptotic to the local sink P_{1+} .

In section 3.2 we derived the leading terms of a series expansions of y_c for each of the above four classes of orbits. We now derive a full series for y_c as given by (54), by giving a series expansion for $I(T)$, first in powers of T and then in powers of $1 - T$. It follows from (53) that (see e.g. [1])

$$I(T) = \frac{2}{5} T^{5/6} {}_2F_1\left(\frac{1}{3}, \frac{5}{6}; \frac{11}{6}; T\right) = \frac{2}{5} T^{5/6} \sum_{n=0}^{+\infty} \frac{\left(\frac{1}{3}\right)_n \left(\frac{5}{6}\right)_n T^n}{\left(\frac{11}{6}\right)_n n!}, \quad (58)$$

where ${}_2F_1$ is the Gaussian hypergeometric function, and $(p)_n$ the Pochhammer symbol, with $(p)_0 = 1$, and $(p)_n = p(p+1)\dots(p+n-1)$, $n \in \mathbb{N}$. A truncated version of (58) when substituted in (54) with $C_- = 0$ yields¹⁴ the leading term expression (39), while if $C_- \neq 0$ we obtain the leading term expression (40) with the arbitrary function C_0 given by $C_0 = C_+/C_-$.

Similarly, we can expand $I(T)$ in powers of $1 - T$ obtaining (see e.g. [1])

$$\begin{aligned} I(T) &= I_1 - \frac{1}{2}(1 - T)^{2/3} {}_2F_1\left(\frac{1}{6}, \frac{2}{3}; \frac{5}{3}; 1 - T\right) \\ &= I_1 - \frac{1}{2}(1 - T)^{2/3} \sum_{n=0}^{+\infty} \frac{\left(\frac{1}{6}\right)_n \left(\frac{2}{3}\right)_n (1 - T)^n}{\left(\frac{5}{3}\right)_n n!}. \end{aligned} \quad (59)$$

A truncated version of (59) in (54) with $C_+I_1 + C_- = 0$ yields the expression (42), while if $C_+I_1 + C_- \neq 0$ we obtain the expression (43) with the arbitrary function C_1 given by $C_1 = C_+/(C_+I_1 + C_-)$.

We can also use the solution for y_c to obtain an explicit expression for y_v , as follows. The GR Poisson equation and the conservation of momentum equation are

¹⁴Making this transition is made somewhat complicated by the fact the series for $I(T)$ is in the denominator of y_c . Truncate the series after three terms if $C_- = 0$ and after one term otherwise.

given by

$$\delta_v = (1+q)^{-1} \mathcal{H}^{-2} \mathbf{D}^2 \psi_p, \quad (60a)$$

$$\delta'_v = -\mathcal{H}^{-2} \mathbf{D}^2 (\mathcal{H} V_p), \quad (60b)$$

respectively, see [22]. In addition we have the relations¹⁵

$$\psi_p = -\mathcal{H} B_c, \quad \mathcal{H} V_p = \mathcal{H} V_c - \mathcal{H} B_c, \quad \phi_c = -(1+q) \mathcal{H} V_c, \quad (61)$$

which lead to the following result:

$$y_v = \frac{\delta'_v}{\delta_v} = \frac{\mathbf{D}^2(-\phi_c)}{\mathbf{D}^2(\mathcal{H} B_c)} - (1+q). \quad (62)$$

We substitute the explicit solution (52) into (62) to obtain

$$y_v(N, x^i) = \frac{(\mathbf{D}^2 C_+) T^{\frac{5}{6}} (1-T)^{\frac{2}{3}}}{(\mathbf{D}^2 C_+) I + (\mathbf{D}^2 C_-)} - \frac{3}{2} (1-T), \quad (63)$$

which for the growing mode ($C_- = 0$) reduces to

$$y_v = T^{\frac{5}{6}} (1-T)^{\frac{2}{3}} I^{-1} - \frac{3}{2} (1-T). \quad (64)$$

It follows from (54) with $C_- = 0$ that for this special orbit we have the simple relation

$$y_v = y_c - \frac{3}{2} (1-T). \quad (65)$$

This relation then establishes that the heteroclinic orbit $P_{0+} \rightarrow P_{1+}$ in both systems represents the same solution, i.e., the growing mode solution. Making a Fourier decomposition of $\mathcal{H} B_c$ and ϕ_c results in that equation (62) also reduces to (65). This explains why making the above variable transformation transforms the system (34) to the system (35).

We conclude by remarking that the explicit solutions makes it possible to give an analytic example of how the growing mode solution acts as an ‘‘attractor solution’’ by defining

$$\delta y_c = y_c - y_c[G] = -\frac{C_- T^{\frac{5}{6}} (1-T)^{\frac{2}{3}}}{I(C_+ I + C_-)}, \quad (66)$$

as follows from equation (54) where $y_c[G]$ stands for the growing mode solution with $C_- = 0$. This is an analytic description of the deviation of solutions from the growing mode solution, which can be given in terms of the redshift z since $T = T(z)$. Finally, note that it is possible for the spatial function C_- to be zero at one, two or three spatial coordinates. This gives rise to a so-called permanent spike, which is an asymptotic spatial discontinuity on a surface, line, or point, respectively, a situation that can be compared with the features of the special explicit solutions of the Einstein field equations given in [14, 13].

¹⁵The first two are standard change of gauge formulas, see e.g. [24], section 3, and the third is the velocity constraint in the uniform curvature gauge, see [22], equation (54c).

3.4 Approximation methods

We now turn to approximation techniques and make comparisons with the exact results. The motivation for this is to develop increasingly accurate approximation schemes that work for problems that are *not* explicitly solvable. From comparisons with the explicit solution we find that the various series expansions obtained by dynamical systems methods give correct asymptotic approximations for the solution. In the present context it is of particular interest to obtain, preferably globally, or at least for all observable redshifts, accurate approximation for the growing mode solution, especially with methods that can be applied to other problems and dynamical systems.

We can improve the accuracy of the previous truncated series approximations by using them to derive Padé approximants.¹⁶ For example, for the growing mode solution originating from P_{0+} in the $y_v - T$ state space we get the following Padé approximation:

$$y_v \approx [1, 1]_{y_v} = \frac{1 - \frac{3 \cdot 7^2}{11 \cdot 17} T}{1 - \frac{3^2 \cdot 5}{11 \cdot 17} T} = \frac{1 + \frac{2^3 \cdot 5}{11 \cdot 17} \lambda_m x^3}{1 + \frac{2 \cdot 7^1}{11 \cdot 17} \lambda_m x^3}. \quad (67)$$

A completely different global approximation for the growing mode solution can be obtained by observing that it is a slowly varying heteroclinic orbit in $T = \Omega_\Lambda$, or, equivalently Ω_m , as can be seen from figure 2. More precisely, it is a trajectory that bends slightly to the right in figure 2 with respect to the straight line $y_v = 1 - T$ that goes through the fixed points P_{0+} and P_{1+} . This motivates the following variable transformation from y_v to a new function $\gamma(T)$, defined by

$$y_v = (1 - T)^{\gamma(T)}, \quad (68)$$

where $\gamma(T)$ is called the *growth (rate) index* function (for a historical background, see the discussion below). Expressing Equation (34) as a first order differential equation for γ results in

$$3T(1 - T) \ln(1 - T) \frac{d\gamma}{dT} - 3T\gamma + \frac{1}{2}(1 + 3T) + (1 - T)^\gamma - \frac{3}{2}(1 - T)^{1-\gamma} = 0, \quad (69)$$

where a power series expansion of $\gamma(T)$ in T yields

$$y_v = (1 - T)^{\frac{6}{11} + \frac{3 \cdot 5}{11^2 \cdot 17} T + \mathcal{O}(T^2)}. \quad (70)$$

Background models with different Ω_{m0} and $\Omega_{\Lambda0}$, i.e., different $\lambda_m = \Omega_{\Lambda0}/\Omega_{m0}$, all have the same trajectories in the dynamical systems pictures. However, when e.g. y_v is plotted against the redshift z , a given solution in the dynamical systems picture, e.g. the growing mode solution, results in a one-parameter set of solutions parameterized by λ_m since

$$z = -1 + \left(\lambda_m \frac{1 - T}{T} \right)^{\frac{1}{3}} = -1 + \left(\lambda_m \frac{\Omega_m}{1 - \Omega_m} \right)^{\frac{1}{3}}. \quad (71)$$

¹⁶For a discussion of Padé approximants in a cosmological setting and further references, see e.g. [2].

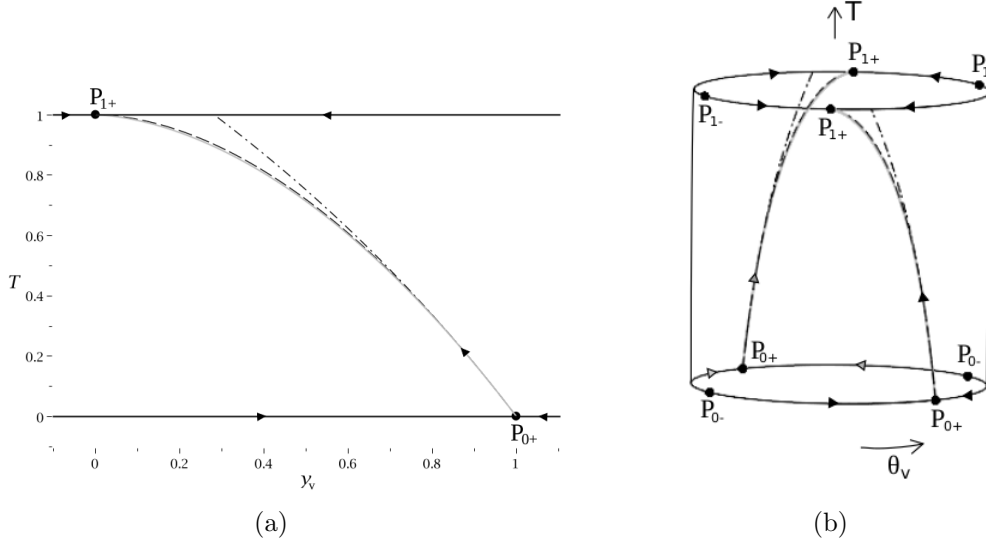
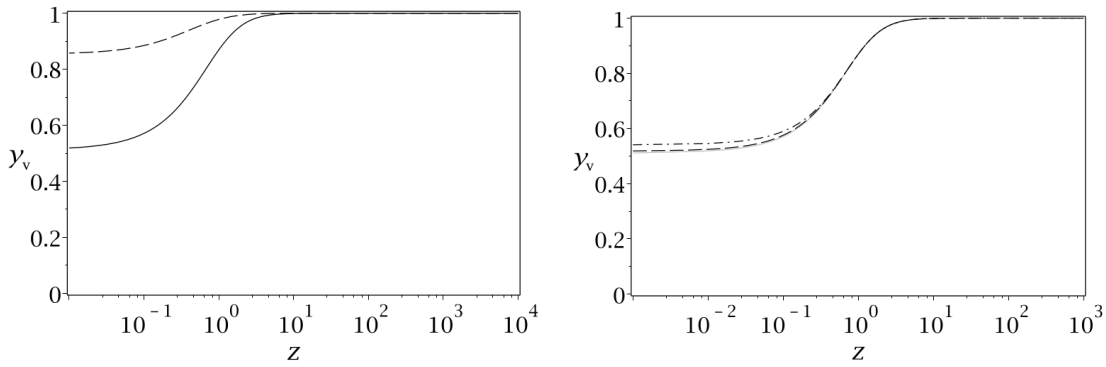


Figure 3: Explicit growing mode solution (solid grey line), the $[1, 1]_{y_v}$ Padé approximant (dashed-dotted), $y_v = (1 - T)^{\frac{6}{11}} = \Omega_m^{\frac{6}{11}}$ (dashed).

The growing mode solution together with the $y_v = [1, 1]_{y_v}$ Padé approximant and the approximation $y_v = (1 - T)^{\frac{6}{11}} = \Omega_m^{\frac{6}{11}}$ are depicted in a redshift diagram in figure 4 for $\lambda_m = 7/3$, i.e., $\Omega_{m0} = 0.3$, $\Omega_{\Lambda 0} = 0.7$ (chosen for simplicity and in agreement with recent observational data, see e.g. [6]), and $\lambda_m = 1/3$, i.e., $\Omega_{m0} = 0.75$, $\Omega_{\Lambda 0} = 0.25$.



(a) The explicit growing mode solution for $\lambda_m = \frac{7}{3}$ (solid) and the one for $\lambda_m = \frac{1}{3}$ (dashed). (b) The explicit growing mode solution for $\lambda_m = \frac{7}{3}$ (grey) and its $[1, 1]_{y_v}$ Padé approximant (dashed-dotted) and the approximation $y_v = (1 - T)^{\frac{6}{11}} = \Omega_m^{\frac{6}{11}}$ (dashed).

Figure 4: Plots of the growing mode solution for y_v as function of the redshift $z = -1 + \left(\lambda_m \frac{1-T}{T}\right)^{\frac{1}{3}} = -1 + \left(\lambda_m \frac{\Omega_m}{1-\Omega_m}\right)^{\frac{1}{3}}$, $\lambda_m = \Omega_{\Lambda 0}/\Omega_{m0}$.

Historically the type of analytical approximation given in equation (70) can be traced back to Peebles [16], which gave it in the form $y_{v0} = \Omega_{m0}^{0.6}$ as an approximation at the present time. For models containing negative curvature Ω_k , a similar approxi-

mation was given by Lightman and Schechter [12], with $y_{v0} = \Omega_{m0}^{\frac{4}{7}}$, see also [5]. Lahav *et al.* [11] realized that this type of approximations could be extended to general redshift z , and they further refined it according to

$$y_v(z) = \Omega_m^{0.6} + \frac{1}{70} \left(1 - \frac{1}{2}\Omega_m(1 + \Omega_m)\right), \quad (72)$$

where

$$\Omega_m = \frac{\Omega_{m0}(1+z)^3}{\Omega_{\Lambda0} + \Omega_{m0}(1+z)^3}, \quad \Omega_{\Lambda0} + \Omega_{m0} = 1. \quad (73)$$

Later Wang and Steinhardt [26], see also references therein, clarified that the values 0.6 and $\frac{4}{7}$ are approximations to $\frac{6}{11}$, obtained by the series expansion given in (70); see also [17] for the correct next order term in the exponent for Λ CDM, which is given in equation (70). The approximations in equation (72), $y_v = (1 - T)^{\frac{6}{11}} = \Omega_m^{\frac{6}{11}}$, and $y_v = \Omega_m^{\frac{6}{11} + \frac{3.5}{11^2 \cdot 17}(1 - \Omega_m)}$ are quite good when compared with the explicit solution (63), as shown by plotting the errors $\Delta = y_v[\text{Approx.}] - y_v[\text{Explicit}]$, i.e. the difference between an approximation and the explicit solution (63), in figure 5(a). For another discussion about approximations, see [10]. Let us now introduce the following simple, admittedly *ad hoc*, correction to $y_v = \Omega_m^{\frac{6}{11}}$, which compensates for the errors for the intermediate evolution,

$$y_v = f = (1 - T)^{\frac{6}{11}} - \frac{1}{70}T^{\frac{5}{2}} = \Omega_m^{\frac{6}{11}} - \frac{1}{70}(1 - \Omega_m)^{\frac{5}{2}}, \quad (74)$$

where the range of z is determined by $T < T_0 = \Omega_{\Lambda0} \approx 0.7$. As seen in figure 5(b), equation (74) is an approximation which is more accurate than $y_v = \Omega_m^{\frac{6}{11} + \frac{3.5}{11^2 \cdot 17}(1 - \Omega_m)}$ by several orders of magnitude for all observational z . It is possible to improve the accuracy further, but we have not been able to do so significantly with an approximation that is as simple or simpler than the present one. It should be noted that all approximations are quite good for large z , i.e., small T ; the differences reside in values for z that are relevant for large scale structure formation at comparatively late times.

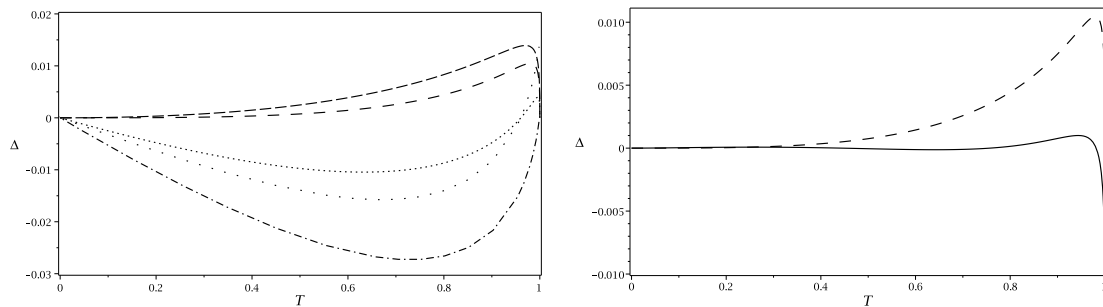
4 Tensor perturbations

Linear tensor perturbations of the spatially flat RW background geometry are characterized by a perturbed metric of the form

$$ds^2 = a^2 \left(-d\eta^2 + (\gamma_{ij} + h_{ij})dx^i dx^j\right), \quad (75)$$

where h_{ij} is a gauge invariant that satisfies $\gamma^{ij}h_{ij} = 0$, $\mathbf{D}^i h_{ij} = 0$. In the absence of anisotropic stresses the perturbed Einstein equations assume the following form (*e.g.* Malik and Wands (2009) [15], equation (8.6)):

$$\partial_\eta^2 h_{ij} + 2\mathcal{H}\partial_\eta h_{ij} - \mathbf{D}^2 h_{ij} = 0. \quad (76)$$



(a) Error plots of previously existing approximations

(b) Error plot comparing the previous best approximation with the new approximation

Figure 5: Error plots $\Delta = y_v[\text{Approx.}] - y_v[\text{Explicit}]$, where $y_v = f(z) = \frac{d \ln \delta}{d \ln a}$, for the approximations: $y_v = \Omega_m^{0.6} + \frac{1}{70} \left(1 - \frac{1}{2} \Omega_m (1 + \Omega_m)\right)$ (spacedot), $y_v = \Omega_m^{\frac{6}{11}}$ (dashed), $y_v = \Omega_m^{\frac{6}{11} + \frac{3.5}{11^2 \cdot 17} (1 - \Omega_m)}$ (spacedash), in figure (a) and (b), $y_v = \Omega_m^{\frac{6}{11}} - \frac{1}{70} (1 - \Omega_m)^{\frac{5}{2}}$ (solid), in figure (b). Note that $T = 1 - \Omega_m = \Omega_\lambda$.

This equation is now going to be used to illustrate the general discussion in section 2 in more detail. In order to formulate this equation as a dynamical system we first introduce e -fold time, which yields

$$h''_{ij} + (2 - q)h'_{ij} - \mathcal{H}^{-2} \mathbf{D}^2 h_{ij} = 0. \quad (77)$$

Using spatial Cartesian coordinates we apply the Fourier transform to this partial differential equation and write the transform of h_{ij} as a linear combination of time-independent polarization tensors e_{ij}^+ and e_{ij}^\times .¹⁷

$$h_{ij}(N, x^i) \longrightarrow h^+(N, k^2) e_{ij}^+ + h^\times(N, k^2) e_{ij}^\times, \quad \mathbf{D}^2 \longrightarrow -k^2, \quad (78)$$

where k is the wave number, and h^+, h^\times are complex-valued functions. The outcome is that each of the functions h^+, h^\times satisfy the following ordinary differential equation:

$$h'' + (2 - q)h' - \mathcal{H}^{-2} k^2 h = 0. \quad (79)$$

In the rest of this section the complex-valued function $h(N, k^2)$ will denote either h^+ or h^\times and we will usually not indicate the dependence on the wave number k explicitly. We finally specialize this differential equation to the Λ CDM universe using (17b), (18) and, (20) to obtain

$$h'' + \frac{3}{2}(2 - \Omega_m)h' + k_0^2 (\lambda_m^{\frac{1}{3}} x) \Omega_m h = 0, \quad (80)$$

where we have introduced a scaled wave number according to $k_0^2 = k^2 / (\lambda_m^{\frac{1}{3}} \Omega_{m0} \mathcal{H}_0^2)$.

The final step in constructing a dynamical system (a system of first order autonomous differential equations) is to follow the approach used for the density perturbation and introduce a (real-valued) quotient variable analogous to y_v . However, since h in (80) is complex and stands for one of the two functions h^+, h^\times , we must

¹⁷See, e.g., Weinberg (2008) [27], page 232 for more detail.

write $h^+ = h_1^+ + ih_2^+$, and $h^\times = h_1^\times + ih_2^\times$ where $h_1^+, h_2^+, h_1^\times, h_2^\times$ are four real-valued functions which independently satisfy (80). Then for any one of these four functions, which we simply denote by $h = h(N, k^2)$, we define

$$y_t(N, k^2) = \frac{h'}{h}. \quad (81)$$

To complete the process we have to choose a suitable time function T . Considerations of the temporally x -dependent functions in the system of perturbative ODEs in order to obtain a regular dynamical system result in a different T than for scalar perturbations, namely¹⁸

$$T = \frac{\lambda_m^{\frac{1}{3}} x}{1 + \lambda_m^{\frac{1}{3}} x}. \quad (82)$$

We now calculate y'_t by differentiating (81) and using (80) and T' by differentiating (82). After expressing the coefficients in terms of T using (20) and (82) we obtain

$$y'_t = - (k_0^2 F(T) + G(T) y_t + y_t^2), \quad (83a)$$

$$T' = T(1 - T), \quad (83b)$$

where

$$F(T) = \lambda_m^{\frac{1}{3}} x \Omega_m = \frac{T(1 - T)^2}{T^3 + (1 - T)^3}, \quad (83c)$$

$$G(T) = \frac{3}{2}(2 - \Omega_m) = \frac{3}{2} \left[\frac{2T^3 + (1 - T)^3}{T^3 + (1 - T)^3} \right]. \quad (83d)$$

Thus equation (83) describes a one-parameter family of real-valued analytic dynamical systems labelled by the parameter k_0^2 , which yields the long wavelength approximation when $k_0^2 = 0$. The state space is again the infinite strip defined by $-\infty < y_t < \infty$, $0 \leq T \leq 1$, which is to be traversed twice in order to describe the global state space of θ_t and T .

The structure of the orbits of this system is very similar to that of the system (35), with the fixed points lying on the boundaries $T = 0$ and $T = 1$. We note that the fixed points do not depend on the arbitrary parameter k_0^2 , since on the boundaries the function $F(T)$ equals zero. When specialized to these boundaries the differential equation (44a) results in the following equations:

$$y'_t|_{T=0} = -y_t \left(\frac{3}{2} + y_t \right), \quad (84a)$$

$$y'_t|_{T=1} = -y_t (3 + y_t). \quad (84b)$$

It follows that on the $T = 0$ boundary the fixed points are given by

$$P_{0+}: \quad y_t = 0; \quad \theta_t = n\pi, \quad (85a)$$

$$P_{0-}: \quad y_t = -\frac{3}{2}; \quad \theta_t = -\arctan \frac{3}{2} + n\pi. \quad (85b)$$

¹⁸Compare with (10) and (27).

Linearization shows that the fixed point P_{0+} is a hyperbolic saddle and that a single orbit originates from P_{0+} and is future asymptotic to the $T = 1$ boundary. This special orbit is approximated by

$$\begin{aligned} y_t &= -\frac{2}{5}k_0^2T - \frac{2}{5}k_0^2\left(1 + \frac{2^2}{5.7}k_0^2\right)T^2 + \dots \\ &= -\frac{2}{5}k_0^2\lambda_m^{\frac{1}{3}}x - \frac{2^3}{5^2.7}\left(k_0^2\lambda_m^{\frac{1}{3}}x\right)^2 + \dots \end{aligned} \quad (86)$$

Next, linearization shows that the fixed point P_{0-} is a hyperbolic source, and hence a one-parameter family of orbits originates from P_{0-} . A series expansion in T results in

$$\begin{aligned} y_t &= -\frac{3}{2} + 2k_0^2T + C_0T^{\frac{3}{2}} + \dots \\ &= -\frac{3}{2} + 2k_0^2\left(\lambda_m^{\frac{1}{3}}x\right) + C_0\left(\lambda_m^{\frac{1}{3}}x\right)^{\frac{3}{2}} \dots, \end{aligned} \quad (87)$$

where C_0 parameterizes the different orbits.

On the $T = 1$ boundary the fixed points are as follows:

$$P_{1+}: \quad y_t = 0; \quad \theta_t = n\pi, \quad (88a)$$

$$P_{1-}: \quad y_t = -3; \quad \theta_t = -\arctan 3 + n\pi. \quad (88b)$$

Linearization shows that the fixed point P_{1-} is a hyperbolic saddle that attracts a single orbit that is past asymptotic to $T = 0$. A series expansion in $1 - T$ yields:

$$\begin{aligned} y_t &= -3 + \frac{k_0^2}{5}(1 - T)^2 + \left(\frac{3}{4} + \frac{2k_0^2}{5}\right)(1 - T)^3 + \dots \\ &= -3 + \frac{k_0^2}{5}\left(\lambda_m^{\frac{1}{3}}x\right)^{-2} + \frac{3}{4}\left(\lambda_m^{\frac{1}{3}}x\right)^{-3} + \dots \end{aligned} \quad (89)$$

Finally, linearization shows that the fixed point P_{1+} is a hyperbolic sink, which implies that a one-parameter family of orbits is asymptotic to P_{1+} . A series expansion in $1 - T$ results in

$$\begin{aligned} y_t &= -k_0^2(1 - T)^2 + C_1(1 - T)^3 + \dots \\ &= -k_0^2\left(\lambda_m^{\frac{1}{3}}x\right)^{-2} + (2k_0^2 + C_1)\left(\lambda_m^{\frac{1}{3}}x\right)^{-3} + \dots, \end{aligned} \quad (90)$$

where C_1 parameterizes the different orbits.

The orbit structure for tensor perturbations for Λ CDM cosmology for a variety of values of k_0 is illustrated in figure 6. Note that for large k_0 , i.e., $k_0 \gg 0$, orbits start to circulate the state space at an intermediate stage of the evolution. This regime is approximately described by the short wavelength limit for dust, but eventually the cosmological constant starts to dominate and the future asymptotic limits for the orbits $y_t(N, k_0^2)$ are the same for all values of k_0 , since the fixed points at $T = 1$ are independent of k_0 .

The long wavelength limit corresponds to $k_0 = 0$ and yields an explicit orbit, which is most conveniently expressed by using

$$\Omega_\Lambda = \frac{\lambda_m x^3}{1 + \lambda_m x^3} = \frac{T^3}{T^3 + (1 - T)^3}, \quad (91)$$

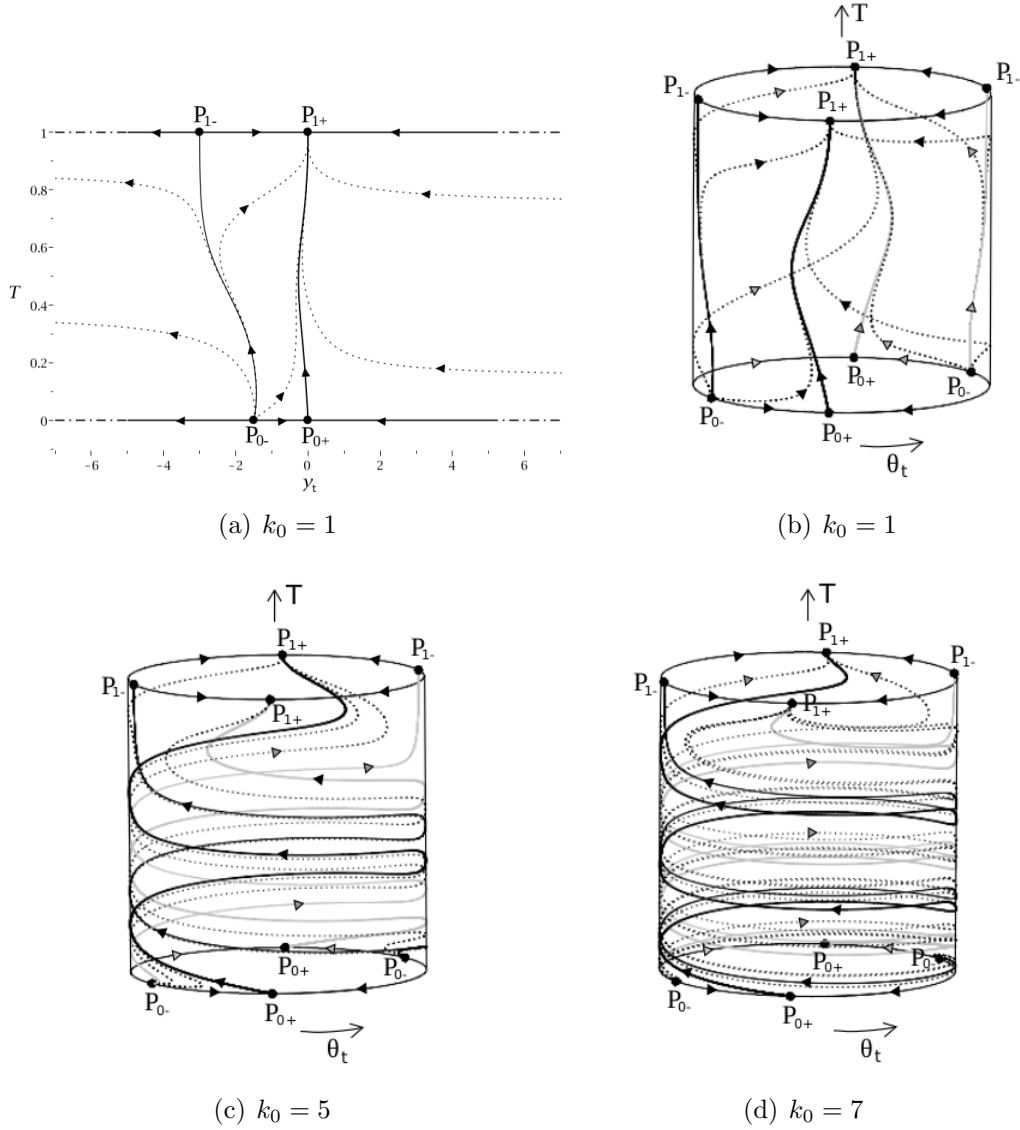


Figure 6: Solution structure for tensor perturbations for Λ CDM cosmology for a variety of values of k_0 .

and is given by

$$y_t = -\frac{(1 - \Omega_\Lambda)C_+}{C_+ + C_- \Omega_\Lambda^{\frac{1}{2}}}. \quad (92)$$

In this case there are two special orbits, one with $C_+ = 0$ going from P_{0+} to P_{1+} and one with $C_- = -C_+$, for which $y_t = -(1 + \Omega_\Lambda^{\frac{1}{2}})$, going from P_{0-} to P_{1-} . The structure of the orbits in the long wavelength limit is illustrated in figure 7.

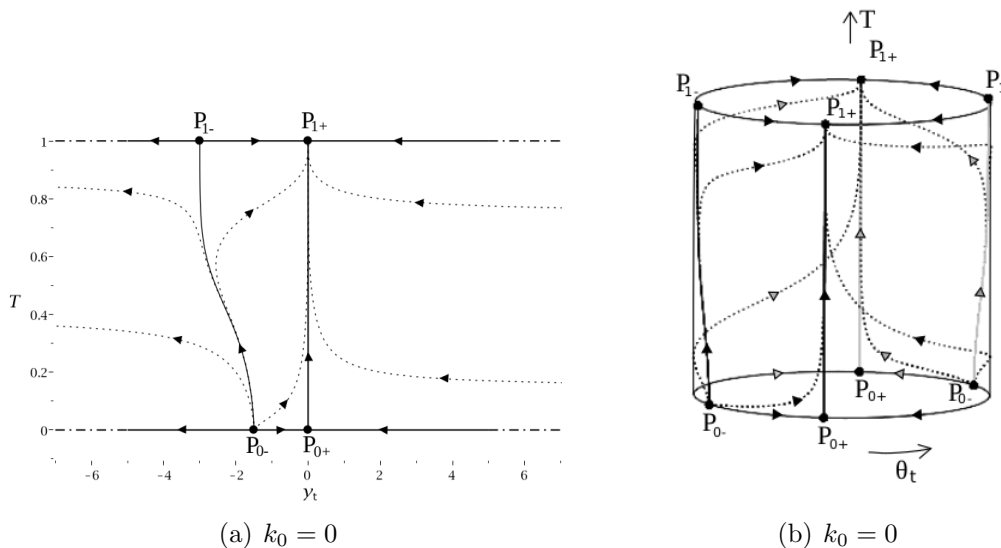


Figure 7: Solution structure for tensor perturbations for Λ CDM cosmology for the long wavelength limit $k_0 = 0$.

5 Measures of anisotropy: the shear and Weyl tensors

In this paper we have given a global analysis of the evolution of linear scalar and tensor perturbations of a Λ CDM universe by formulating the perturbed Einstein equations as dynamical systems. In order to place this analysis in perspective we now consider the family of solutions of the Einstein equations whose matter content is irrotational dust and a cosmological constant. These solutions model a class of universes that generalize the Λ CDM universe which is the unique model in this class that describes a completely isotropic universe with flat spatial geometry. We will thus refer to these universes as generalized Λ CDM universes. Complete isotropy is characterized by the requirement that the shear tensor σ^a_b of the fluid congruence and the Weyl curvature tensor C^{ab}_{cd} are zero. From an observational point of view one is interested in universes in which the anisotropy is small, by which one means that the shear tensor and the Weyl tensor are small relative to the overall expansion of the universe, described by the Hubble scalar H . We thus form dimensionless scalars by normalizing the contracted shear and Weyl tensors¹⁹ with an appropriate power of the Hubble scalar H :

$$\Sigma^2 = (\sigma^a_b \sigma^b_a) / H^2, \quad C^2 = (C^{ab}_{cd} C^{cd}_{ab}) / H^4. \quad (93)$$

There exists a number of results about the evolution of generalized Λ CDM universes. First, as regards late times it has been shown that universes in this family

¹⁹One can decompose the Weyl tensor into an electric and magnetic part relative to a given timelike congruence, with spatial components denoted $C^{n_i}_{\eta_j}$ and $C^{n_i}_{lm} \varepsilon^{lm}_j$, where ε_{ijk} is the three dimensional alternating symbol. One can form space-time scalars using C^{ab}_{cd} as below, or spatial scalars using the electric and magnetic parts.

that expand indefinitely approach the de Sitter model for an open set of initial conditions,²⁰ in the sense that

$$\lim_{x \rightarrow \infty} \Sigma^2 = 0, \quad \lim_{x \rightarrow \infty} C^2 = 0, \quad \lim_{x \rightarrow \infty} \Omega_m = 0, \quad (94)$$

Second it has been shown that there is a subset of models which approximate the flat Friedmann-Lemaître model on approach to the singularity,²¹

$$\lim_{x \rightarrow 0} \Sigma^2 = 0, \quad \lim_{x \rightarrow 0} C^2 = 0, \quad \lim_{x \rightarrow 0} \Omega_m = 1. \quad (95)$$

The singularity in these models is referred to as an isotropic singularity (see Goode and Wainwright (1985) [7]). On the other hand a typical model undergoes a more complicated evolution described by BKL oscillations and possible so-called spike oscillations on approach to the singularity (see e.g. [19]). Nevertheless, the Hubble-normalized anisotropy scalars Σ^2 and C^2 remain bounded during this process, a result that we will use later in this section.

In this paper we have illustrated the global solution space of the linearly perturbed Λ CDM models using dynamical systems that describe scalar and tensor perturbations separately. We will now use the shear and Weyl tensors to compare the asymptotic behaviour of the perturbations at early and late times with the full state space picture of Einstein's field equations in the Hubble-normalized state space description given in [14], and briefly described above.

We refer to [20] for expressions for the perturbed shear and Weyl tensors.²² For the linear scalar and tensor perturbations the perturbed shear tensor is given by

$$\frac{{}^{(1)}\sigma_i^j}{H} = \mathcal{H}^{-2} \mathbf{D}_j^i (\mathcal{H}V_p) + \frac{1}{2} \partial_N h_j^i, \quad (96a)$$

while the perturbed electric Weyl tensor is given by²³

$$\frac{{}^{(1)}C^{\eta j}_{\eta i}}{H^2} = -\mathcal{H}^{-2} (\mathbf{D}_j^i \psi_p) + (\partial_N - \mathcal{H}^{-2} \mathbf{D}^2) h_j^i. \quad (96b)$$

5.1 Scalar perturbations

We apply the scalar mode extraction operator \mathcal{S}^{ij} , given in Appendix A in [21], to form the shear and electric Weyl scalars. After using the relations

$$\mathcal{H}V_p = \psi_p + \mathcal{H}V_c, \quad \psi_p = -\mathcal{H}B_c, \quad \mathcal{H}V_c = -(1+q)^{-1} \phi_c. \quad (97)$$

²⁰This class of cosmologies is labelled by eight arbitrary spatial functions, Lim *et al.* (2004) [14], page 8.

²¹This class of cosmologies is labelled by three arbitrary spatial functions [14], page 11.

²²See equations (B35a) and (B41c), which we specialize as follows. We assume zero anisotropic stress, which implies $\Psi = \Phi$, a flat background ($K = 0$) and for simplicity we exclude the vector mode ($\mathbf{B}_i = 0$). Note that the present $h_{ij} = \frac{1}{2} \mathbf{C}_{ij}$.

²³One can give a similar expression for the perturbed magnetic Weyl tensor, but we have found that it has similar asymptotic properties as the electric Weyl tensor.

we obtain:

$$\Sigma_s \equiv \frac{\mathcal{S}_j^{i(1)}\sigma_i^j}{H} = -\mathcal{H}^{-2} \left((1+q)^{-1}\phi_c + \mathcal{H}B_c \right), \quad (98a)$$

$$W_s \equiv \frac{\mathcal{S}_j^{i(1)}C^{nj}_{ni}}{H^2} = \mathcal{H}^{-2}(\mathcal{H}B_c). \quad (98b)$$

In the dynamical systems formulation for the scalar perturbations we have chosen a variable T according to equation (27) which yields $1+q = \frac{3}{2}(1-T)$ and

$$\mathcal{H}^{-2} = (\mathcal{H}_0)^{-2} \left(\frac{1+\lambda_m}{\lambda_m^{1/3}} \right) T^{1/3}(1-T)^{2/3}. \quad (99)$$

One can express Σ_s and W_s in the non-reduced state space $(\mathcal{H}B_c, y_c, T)$, which yields

$$\Sigma_s = -\mathcal{H}^{-2}(1+q)^{-1}(\mathcal{H}B_c)(1+q-y_c), \quad W_s = \mathcal{H}^{-2}(\mathcal{H}B_c). \quad (100)$$

Using the previously obtained asymptotic expressions for y_c and inserting them into equation (30) for $\mathcal{H}B_c$ to obtain asymptotic expressions for $\mathcal{H}B_c$ subsequently results in asymptotic expressions when $T \rightarrow 0$ and $T \rightarrow 1$ for Σ_s and W_s . However, since we in the present case have explicit solutions for ϕ_c and $\mathcal{H}B_c$, given in equation (52), we can give explicit expressions for Σ_s and W_s as functions of T :

$$\Sigma_s \propto T^{\frac{1}{3}}(1-T)^{\frac{2}{3}}C_+ - \frac{3}{2}T^{-\frac{1}{2}}(1-T)(C_+I + C_-), \quad (101a)$$

$$W_s \propto \frac{3}{2}T^{-\frac{1}{2}}(1-T)(C_+I + C_-), \quad (101b)$$

where we recall that $T = \lambda_m x^3 / (1 + \lambda_m x^3)$. It follows that

$$\lim_{x \rightarrow 0} |\Sigma_s| = \infty, \quad \text{if } C_- \neq 0, \quad \lim_{x \rightarrow 0} \Sigma_s = 0, \quad \text{if } C_- = 0, \quad (102)$$

where the second result follows from $I \propto T^{\frac{5}{6}}$ when $T \rightarrow 0$. The Weyl scalar has the same limits. One can also infer the asymptotic rate of growth/decay of Σ_s and W_s as $x \rightarrow 0$ from equation (101):

$$\Sigma_s, W_s \propto x^{-3/2}, \quad \text{if } C_- \neq 0, \quad \Sigma_s, W_s \propto x, \quad \text{if } C_- = 0. \quad (103)$$

The limits (102) suggest that the growing mode (the orbit past asymptotic to the fixed point P_{0+} , given by $C_- = 0$), approximates an exact solution with an isotropic singularity. The asymptotic decay rate in (103) agrees with the asymptotic results of Lim *et al.* (2004) [14] (see equations (4.19) and (5.9)). On the other hand, the unboundedness of the Hubble-normalized shear perturbation when $C_- \neq 0$ indicates that generic perturbations become physically unviable, *i.e.* do not approximate exact solutions of the Einstein field equations, when T is sufficiently close to zero.

One can also use (101) to determine the asymptotic behaviour of Σ_s and W_s at late times ($T \rightarrow 1, x \rightarrow \infty$). Since $\lim_{x \rightarrow \infty} I$ is finite it follows that

$$\lim_{x \rightarrow \infty} (\Sigma_s, W_s) = 0, \quad (104)$$

for all C_+, C_- . Equation (101) also gives the rates of decay along generic orbits asymptotic to the fixed point $P_{1+}(C_+I_1 + C_- \neq 0)$:

$$\Sigma_s = \mathcal{O}(x^{-2}), \quad W_s = \mathcal{O}(x^{-3}). \quad (105)$$

The result (104) for perturbations of Λ CDM is compatible with the future asymptotic behaviour of generalized Λ CDM universes toward a future de Sitter state, as described by equation (94), where equation (105) agrees with the asymptotic results of Lim *et al* (2004) [14] (see equations (3.24) and (5.8)).

5.2 Tensor perturbations

To analyze the tensor perturbations we make the transition (78) to Fourier space and use one of the four real-valued functions h to represent the perturbation. Thus according to (96) the shear will be represented by $\frac{1}{2}h'$ and the electric Weyl tensor will be represented by $\frac{1}{2}(h' - k^2\mathcal{H}^{-2}h)$, which motivates defining the shear scalar and electric Weyl scalar for tensor perturbations according to

$$\Sigma_t = \frac{1}{2}h', \quad W_t = \frac{1}{2}(h' - k^2\mathcal{H}^{-2}h), \quad (106)$$

where

$$\mathcal{H}^{-2} = (\mathcal{H}_0)^{-2} \left(\frac{1 + \lambda_m}{\lambda_m^{1/3}} \right) \frac{\lambda_m^{1/3}x}{1 + \lambda_m x^3}, \quad T = \frac{\lambda_m^{1/3}x}{1 + \lambda_m^{1/3}x}. \quad (107)$$

In order to analyze the behaviour of these scalars along the orbits we first rewrite the defining equation $y_t = h'/h$ in the form $d(\ln h)/dT = y_t dN/dT = y_t/(T(1-T))$ and then integrate to obtain

$$h(T) = h_0 \exp \left(\int_{T_0}^T \frac{y_t(\tilde{T})}{\tilde{T}(1-\tilde{T})} d\tilde{T} \right). \quad (108)$$

It then follows from (106) that Σ_t and W_t are given as functions of T along the orbits by

$$\Sigma_t(T) = \frac{1}{2}h(T)y_t(T), \quad W_t(T) = \frac{1}{2}h(T)(y_t(T) - k^2\mathcal{H}^{-2}(T)). \quad (109)$$

We can now use the asymptotic expansions for the four fixed points in the previous section to determine the asymptotic form of $h(t)$ and hence of Σ_t . We first consider the orbits that are past asymptotic to P_{0+} and P_{0-} as $T \rightarrow 0$ ($x \rightarrow 0$), referring to equations (86) and (87):

$$P_{0+}: \quad y_t = \mathcal{O}(T), \quad T \rightarrow 0 \quad \Rightarrow \quad \lim_{T \rightarrow 0} h(T) \neq 0 \quad \Rightarrow \quad \lim_{x \rightarrow 0} \Sigma_t = 0, \quad (110a)$$

$$P_{0-}: \quad y_t \approx -\frac{3}{2}, \quad T \rightarrow 0 \quad \Rightarrow \quad \lim_{T \rightarrow 0} h(T) = \infty \quad \Rightarrow \quad \lim_{x \rightarrow 0} \Sigma_t = \infty. \quad (110b)$$

One can further obtain the leading temporal x -dependence, as follows:

$$P_{0+}: \Sigma_t = \mathcal{O}(x), \quad P_{0-}: \Sigma_t = \mathcal{O}(x^{-3/2}), \quad \text{as } x \rightarrow 0. \quad (111)$$

Since $\mathcal{H}^{-2}(0) = 0$ it follows from (109) that W_t has the same asymptotic behaviour as Σ_t .

The above results describe the asymptotic behaviour of the perturbed shear and electric Weyl scalars near the initial singularity. We see that the results are the same as for scalar perturbations. For example, only the single orbit $P_{0+} \rightarrow P_{1+}$ in figure 6 and figure 7 is compatible with an isotropic singularity and this orbit is thus analogous to the growing mode orbit $P_{0+} \rightarrow P_{1+}$ for scalar perturbations in figure 1.

We now consider the orbits that are future asymptotic to the fixed points P_{1+} and P_{1-} as $T \rightarrow 1$ ($x \rightarrow \infty$), referring to equations (90) and (89):

$$P_{1+}: \quad y_t = \mathcal{O}((1-T)^2), \quad T \rightarrow 1 \quad \Rightarrow \quad \lim_{T \rightarrow 1} h(T) \neq 0 \quad \Rightarrow \quad \lim_{x \rightarrow \infty} \Sigma_t = 0, \quad (112a)$$

$$P_{1-}: \quad y_t \approx -3, \quad T \rightarrow 1 \quad \Rightarrow \quad \lim_{T \rightarrow 1} h(T) = 0 \quad \Rightarrow \quad \lim_{x \rightarrow \infty} \Sigma_t = 0. \quad (112b)$$

One can further obtain the leading x -dependence, as follows:

$$P_{1+}: \quad \Sigma_t = \mathcal{O}(x^{-2}), \quad P_{1-}: \quad \Sigma_t = \mathcal{O}(x^{-3}), \quad \text{as } x \rightarrow \infty. \quad (113)$$

Again, W_t has the same asymptotic behaviour as Σ_t . Here there is one difference between the scalar and tensor perturbations: both Σ_s and Σ_t are $\mathcal{O}(x^{-2})$ as $x \rightarrow \infty$, while W_s is $\mathcal{O}(x^{-2})$ and W_t is $\mathcal{O}(x^{-3})$. Since the asymptotic perturbations agree with the asymptotic results for the full Einstein equations in (94) one expects that the perturbations will approximate exact solutions at late times toward the future asymptotic de Sitter state.²⁴

6 Concluding remarks

In this paper we have presented a dynamical systems approach to linear scalar and tensor perturbations of the Λ CDM model. It has been shown that it is only solutions that originate from a fixed point P_{0+} in both the scalar and tensor perturbation dynamical systems that asymptotically toward the past correspond to solutions of the Einstein field equations, namely solutions that have an isotropic singularity. As a consequence, at early times, only initial data that are sufficiently close to the fixed point P_{0+} , for both modes, are physically relevant. Moreover, in both the scalar and tensor cases the fixed point P_{0+} is a saddle, and as a consequence solutions near the fixed point P_{0+} are ‘‘attracted’’ to the $P_{0+} \rightarrow P_{1+}$ orbit in both cases (the growing mode solution in the scalar mode case) and therefore also end at the future attractor P_{1+} . These conclusions can be reached by considering the asymptotics obtained by means of dynamical systems analysis and by considering the Hubble-normalized fluid shear and Weyl scalars. This will be the strategy when considering

²⁴As regards fluids with rotation, vector perturbations B_i are given by $B_i = b_i x^{-2}$, where b_i depends on the spatial coordinates only, as follows from equation (58a) in [20]. Equations (58b), (42a), (66d) in the same reference yields \tilde{v}_i , which together with B_i when inserted into equation (B.41c) for the vector mode of $({}^1\sigma^i_j/{}^{(0)}H)$ results in that this quantity is $\propto x^{-\frac{3}{2}}$ when $x \rightarrow 0$. Hence the vector modes have to be set to zero in the case of an isotropic singularity. Equation (B.41d) in [20] for the fluid rotation also results in an initial blow up, unless the vector mode is set to zero.

more general models, e.g. models involving scalar fields, which do not admit explicit solutions. In forthcoming work it is also interesting to relate asymptotic results concerning future evolution, obtained by our dynamical systems approaches to scalar and tensor perturbations, to results about global future stability of small non-linear perturbations of Λ CDM models, see [9], as well as to small non-linear perturbations of more general models.

In the next paper we will consider linear perturbations of minimally coupled scalar fields with an exponential potential on a spatially flat background. The reason for considering these models is twofold. First, in the present models the background is rather trivially coupled to the perturbations by a single variable T . This is no longer the case for scalar fields where instead the perturbations are coupled to the background via equations for several background variables, thereby leading to problems with a more complicated state space structure than the presently discussed models. The exponential potential corresponds to a scale-invariant problem and as a consequence only two background variables couple to a reduced perturbation variable y for both scalar and tensor perturbations, resulting in 3-dimensional reduced dynamical systems, which therefore makes it possible to illustrate global dynamics with illustrative pictures. Second, the exponential potential case can be shown to be part of the boundary of dynamical systems of more general problems with non-scale-invariant scalar field potentials. These models thereby play an essential role in investigating such models, and is therefore a next natural step in studying an hierarchy of increasingly complex problems.²⁵

Acknowledgments

AA is funded by the FCT grant SFRH/BPD/85194/2012, and supported by the project (GPSEinstein) PTDC/MAT-ANA/1275/2014, and CAMGSD, Instituto Superior Técnico by FCT/Portugal through UID/MAT/04459/2013. Furthermore, AA thanks the warm hospitality of Karlstad University. CU would like to thank the CAMGSD, Instituto Superior Técnico in Lisbon and the University of Waterloo, Canada, for kind hospitality.

References

- [1] M. Abramowitz and I.A. Stegun. *Handbook of mathematical functions 10th ed.* Dover Publications, 1972.

²⁵In [3] the authors are making broad claims about the non-viability of quintessence as regards the future stability of de Sitter and as deviations from the Λ CDM model. However, they use a dynamical system in which U_m , i.e., y_v , is in the denominator in their equation (27). Since $U_m \rightarrow 0$ for de Sitter, this unfortunately results in that the authors draw erroneous conclusions about scalar field models with positive potentials. A simple example illustrating this is a model with a positive constant potential, which can be interpreted as a stiff fluid model with a cosmological constant. For these models it is known that there exists an open set of solutions that are attracted to a future locally stable de Sitter state. Moreover, since there exist quintessence models with solutions that coincide with the Λ CDM model, clearly there are quintessence models that are as viable as the Λ CDM model. In conclusion, to make correct statements about asymptotic and global behaviour it is essential that the dynamical system is regular on the entire state space.

- [2] A. Alho and C. Uggla. Global dynamics and inflationary center manifold and slow-roll approximants. *Journal of Mathematical Physics*, **56**(012502), 2015.
- [3] S. Basilakos, G. Leon, G. Papagiannopoulos, and E. N. Saridaki. Dynamical system analysis at background and perturbation levels: Quintessence in severe disadvantage comparing to LCDM. *arXiv:1904.01563 [gr-qc]*, 2019.
- [4] M. Bruni and K. Piotrkowska. Dust - radiation universes: Stability analysis. *Mon. Not. Roy. Astron. Soc.*, **270**:630–640, 1994.
- [5] S. M. Carroll, W. H. Press, and E. L. Turner. The cosmological constant. *Ann. Rev. Astron. Astrophys.*, **30**:499–542, 1992.
- [6] Planck Collaboration. Planck 2018 results. VI. cosmological parameters. *arXiv:1807.06209 [astro-ph.CO]*, 2018.
- [7] S. Goode and J. Wainwright. Isotropic singularities in cosmological models. *Class. Quantum Grav.*, **2**:99, 1985.
- [8] H. A. Gressel and M. Bruni. fnl - gnl mixing in the matter density field at higher orders. *JCAP*, (06):016, 2018.
- [9] M. Hadzic and J. Speck. The global future stability of the flrw solutions to the dust-einstein system with a positive cosmological constant. *J. of Hyperbolic Diff. Eq.*, **12**:87, 2015.
- [10] A. J. S. Hamilton. Formulae for growth factors in expanding universes containing matter and a cosmological constant. *Month. Roy. Astron. Soc.*, **322**:419–425, apr 2001.
- [11] O. Lahav, P. B. Lilje, J. R. Primack, and M. J. Rees. Dynamical effects of the cosmological constant. *Month. Roy. Astron. Soc.*, **251**:128–136, jul 1991.
- [12] A. P. Lightman and P. L. Schechter. The omega dependence of peculiar velocities induced by spherical density perturbations. *Astro. Phys. J.*, **74**:831, dec 1990.
- [13] W. C. Lim. The dynamics of inhomogeneous cosmologies. 2004.
- [14] W. C. Lim, H. van Elst, C. Uggla, and J. Wainwright. Asymptotic isotropization in inhomogeneous cosmology. *Phys. Rev.*, **D69**:103507, 2004.
- [15] K. A. Malik and D. Wands. Cosmological perturbations. *Physics Reports*, **475**:1–51, 2009.
- [16] P. J. E. Peebles. *The large-scale structure of the universe*. Princeton University Press, 1980.
- [17] S. Tsujikawa, A. De Felice, and J. Alcaniz. Testing for dynamical dark energy models with redshift-space distortions. *JCAP*, **1301**:030, 2013.

- [18] C. Uggla. Asymptotic cosmological solutions: orthogonal bianchi type-ii models. *Class. Quantum Grav.*, **6**(3):383, 1989.
- [19] C. Uggla. Recent developments concerning generic spacelike singularities. *Gen. Rel. Grav.*, **45**:1669–1710, 2013.
- [20] C. Uggla and J. Wainwright. Cosmological perturbation theory revisited. *Class. Quantum Grav.*, **28**:175017, 2011.
- [21] C. Uggla and J. Wainwright. A simplified structure for the second order cosmological perturbation equations. *Gen. Rel. Grav.*, **45**:643, 2013.
- [22] C. Uggla and J. Wainwright. Second order cosmological perturbations: dynamics. *Phys. Rev. D*, **98**:103534, 2018.
- [23] C. Uggla and J. Wainwright. Second order cosmological perturbations: conserved quantities and explicit solutions at large scales. *e-Print: arXiv:1903.01840 [gr-qc]*, 2019.
- [24] C. Uggla and J. Wainwright. Second order cosmological perturbations: simplified gauge change formulas. *Class. Quantum Grav.*, **36**:035004, 2019.
- [25] J. Wainwright and G. F. R. Ellis. *Dynamical systems in cosmology*. Cambridge University Press, 1997.
- [26] L. Wang and P. J. Steinhardt. Cluster abundance constraints for cosmological models with a time-varying, spatially inhomogeneous energy component with negative pressure. *The Astrophysical Journal*, **508**(2):483, 1998.
- [27] S. Weinberg. *Cosmology*. Oxford university press, 2008.